Pharmacy Faculty Articles and Research   School of Pharmacy

2012

Cytomegalovirus CC Chemokine Promotes Immune Cell Migration

Jennifer Totonchy
Chapman University, totonchy@chapman.edu

Michael Denton
Oregon Health Sciences University,

Craig N. Kreklywich
Portland Veterans Affairs Medical Center

Takeshi Andoh
Portland Veterans Affairs Medical Center

Jessica M. Osborn
Oregon Health Sciences University

See next page for additional authors

Follow this and additional works at: https://digitalcommons.chapman.edu/pharmacy_articles

Part of the Amino Acids, Peptides, and Proteins Commons, Animal Diseases Commons, Complex Mixtures Commons, Hemic and Immune Systems Commons, Other Pharmacy and Pharmaceutical Sciences Commons, and the Virus Diseases Commons

Recommended Citation

Cytomegalovirus CC Chemokine Promotes Immune Cell Migration

Authors

Jennifer Totonchy, Michael Denton, Craig N. Kreklywich, Takeshi Andoh, Jessica M. Osborn, Daniel Chen, Ilhem Messaoudi, Susan L. Orloff, and Daniel N. Streblow

Cytomegalovirus CC Chemokine Promotes Immune Cell Migration

Jennifer Vomaske,[c,d] Michael Denton,[c,d] Craig Kreklywich,[a,b] Takeshi Andoh,[a,b] Jessica M. Osborn,[c,d] Daniel Chen,[c,d] Ilhem Messaoudi,[c,d] Susan L. Orloff,[a,b] and Daniel N. Streblow[c,d]

Portland Veterans Affairs Medical Center, Portland, Oregon, USA,[a] and Departments of Surgery[b] and Molecular Microbiology and Immunology[c] and The Vaccine and Gene Therapy Institute,[d] Oregon Health Sciences University, Portland, Oregon, USA

Cytomegaloviruses manipulate the host chemokine/receptor axis by altering cellular chemokine expression and by encoding multiple chemokines and chemokine receptors. Similar to human cytomegalovirus (HCMV), rat cytomegalovirus (RCMV) encodes multiple CC chemokine-analogous proteins, including r129 (HCMV UL128 homologue) and r131 (HCMV UL130 and MCMV m129/130 homologues). Although these proteins play a role in CMV entry, their function as chemotactic cytokines remains unknown. In the current study, we examined the role of the RCMV chemokine r129 in promoting cellular migration and in accelerating transplant vascular sclerosis (TVS) in our rat heart transplant model. We determined that r129 protein is released into culture supernatants of infected cells and is expressed with late viral gene kinetics during RCMV infection and highly expressed in heart and salivary glands during *in vivo* rat infections. Using the recombinant r129 protein, we demonstrated that r129 induces migration of lymphocytes isolated from rat peripheral blood, spleen, and bone marrow and from a rat macrophage cell line. Using antibody-mediated cell sorting of rat splenocytes, we demonstrated that r129 induces migration of naïve/central memory CD4$^+$ T cells. Through ligand-binding assays, we determined that r129 binds rat CC chemokine receptors CCR3, CCR4, CCR5, and CCR7. In addition, mutational analyses identified functional domains of r129 resulting in recombinant proteins that fail to induce migration (r129-ΔNT and -C31A) or alter the chemotactic ability of the chemokine (r129-F43A). Two of the mutant proteins (r129-C31A and -ΔNT) also act as dominant negatives by inhibiting migration induced by wild-type r129. Furthermore, infection of rat heart transplant recipients with RCMV containing the r129-ΔNT mutation prevented CMV-induced acceleration of TVS. Together our findings indicate that RCMV r129 is highly chemotactic, which has important implications during RCMV infection and reactivation and acceleration of TVS.

In humans and in animal models, cytomegalovirus (CMV) infection accelerates transplant vascular sclerosis (TVS) in solid organ transplantation, resulting in graft failure (7, 18, 19, 24, 26). In our rat heart, kidney, and small bowel transplant models, we have demonstrated that acute infection with rat CMV (RCMV) dramatically decreases the mean time to development of TVS and to graft failure and additionally increases the severity of TVS in grafted vessels (27, 28). chemokines are a group of inducible cytokines that promote cellular migration and activation through binding to their respective G protein-coupled receptors (31). The four classes of chemokines are (i) CC chemokines (monocyte chemotactic protein 1 [MCP-1]), macrophage inflammatory protein 1α [MIP-1α], MIP-1β, and RANTES), (ii) CXC chemokines (interleukin 8 [IL-8], gamma interferon-inducible protein 10 [IP-10], and stromal-cell-derived factor 1α [SDF-1α]), (iii) C chemokines (lymphotactin), and (iv) CX$_3$C chemokines (fractalkine). chemokines play a major role in the development of TVS and chronic rejection. chemokines are upregulated in vascularized grafts at all stages posttransplantation, including ischemia/reperfusion injury, acute rejection, and chronic rejection and during the healing processes (22). In contrast, long-term graft acceptance is associated with the absence of chemokines, thus substantiating a major role for chemokines in allogeneic graft rejection and TVS (32). CC and CXC chemokines have been detected in rejecting human and animal model allografts (22). Importantly, in a mouse heart chronic rejection (CR) transplant model, deletion of CC chemokine receptor 1 (CCR1) or CCR5 resulted in significantly prolonged graft survival (12). Similarly, wild-type (30) mouse heart allograft recipients treated with antibodies directed against CCR5 had delayed acute graft rejection (11). These data suggest

that CC chemokines play a major role in acute rejection, TVS, and CR. In our rat heart transplant model, RCMV-infected allografts, and not uninfected controls, contain immune infiltrates at times paralleling the initial acceleration of TVS (41). This immune cell infiltration is associated with an increased expression of chemokines, including RANTES, MCP-1, MIP1-α, IP-10, fractalkine, and lymphotactin. These data suggest that the link between CMV and TVS involves a complex and dynamic interplay between the virus and host inflammatory response mediated by an increased expression of chemokines.

Herpesvirus subversion of the chemokine network plays an important role in host immune evasion (4, 47). Many herpesviruses, including Kaposi's sarcoma-associated herpesvirus (KSHV) and human CMV (HCMV), encode soluble chemokine-binding proteins that bind to cellular chemokines, thereby reducing chemotaxis of lymphocytes to sites of virus infection (4, 52). In addition, many herpesviruses encode chemokine homologues. Generally, the characterized CMV-encoded chemokine homologues are proinflammatory, suggesting a role in viral dissemination via recruitment of permissive leukocyte or progenitor cell populations to the sites of infection (10, 15, 23, 29, 33, 34). HCMV encodes two CXC chemokine homologues, UL146 and UL147, and one puta-

tive CC chemokine homologue, UL128 (9). The best-characterized CMV chemokine homologue is the murine CMV (MCMV) CC chemokine m131/129 murine chemokine 2 (MCK-2), which is a product of the spliced fusion of the m131 and m129 genes. MCK-2 is a functional chemokine with chemotactic activity *in vivo*. MCK-2 mutant viruses are not defective in virus replication *in vitro*, at the initial sites of infection, or in dissemination to many secondary sites but have been associated with a significant decrease in virus dissemination to the salivary glands (a crucial site for secondary CMV transmission) (10). MCK-2 was shown to specifically recruit immature myelomonocytic leukocytes from bone marrow to the initial sites of MCMV infection (23). The proposed function of MCK-2 is to recruit a mobile leukocyte population to early sites of CMV infection in order to efficiently disseminate the virus to important secondary sites such as the salivary glands. The analogous region in the RCMV genome contains open reading frames (ORFs) colinear to those in MCMV, designated r131 and r129. The gene product of r131 is a homologue of MCK-2. Similar to MCK-2 knockout MCMV strains, recombinant RCMV strains lacking r131 show defects in dissemination to the spleen and salivary glands (15). Sequence alignment indicates that the r131 gene product shares 12% homology to rat CC chemokine MIP-1β, a monocyte chemotactic protein. Unlike m129, which merely donates the sequence for the C terminus of MCK-2 and has no intrinsic CC chemokine characteristics, the putative r129 gene product contains N-terminal CC chemokine consensus sequences, suggesting that RCMV encodes two separate CC chemokine homologues in this region. Interestingly, r129 has significant homology (19.4%) to HCMV UL128, which has been found in clinical strains and is predicted to encode a CC chemokine (1). Detailed characterization of specific chemotactic activities of any of the r131 and r129 gene products or their homologues in HCMV remains to be established.

In the current study, we demonstrated that RCMV r129 is expressed *in vivo* during viral persistence and encodes a functional CC chemokine that is released from infected cells. Recombinant r129 is chemotactic to primary rat lymphocytes and specifically recruits naïve and/or central memory CD4$^+$ T cells. We further identified functional domains of r129 that are critical for migration via site-directed mutagenesis. Binding assays showed that r129 binds CCR3, CCR4, CCR5, and CCR7, which are important chemokine receptors involved in inflammation and allograft rejection. Furthermore, r129 is necessary for the acceleration of TVS based on *in vivo* studies where rat heart allograft recipients infected with RCMV containing the r129-ΔNT mutation failed to accelerate TVS. These findings demonstrate a role for r129 in CMV-accelerated TVS and chronic rejection as well as CMV-mediated promotion of memory T cell inflation by recruiting CD4$^+$ T cells and macrophages.

MATERIALS AND METHODS

Cells and viruses. Rat alveolar macrophages (ATCC NR8383) were maintained in RPMI medium with 10% fetal calf serum (FCS) and penicillin-streptomycin-L-glutamine (PSG; Life Technologies, Grand Island, NY). Primary rat peripheral blood mononuclear cells (PBMC) were isolated by overlaying 6 ml whole blood of F344 adult male rats over 5 ml Ficoll-Paque (GE Healthcare Bio-Sciences, Piscataway, NJ), centrifuging 45 min at 1,500 rpm, and isolating the buffy coat layer. Lymphocytes were washed with phosphate-buffered saline (PBS) and resuspended in RPMI medium without supplements. Primary rat bone marrow cells were isolated by flushing bone marrow from rat femurs and tibias and straining through a 70-μm filter. Bone marrow cells were washed in PBS and resuspended in RPMI medium without supplements. Primary rat splenocytes were isolated via maceration of spleen tissue though a polystyrene mesh followed by lysis of red blood cells (RBC) in 0.84% ammonium chloride for 5 min. RBC lysis was stopped by the addition of an equal volume of RPMI medium with 10% FBS. Splenocytes were then strained through a 70-μm filter and resuspended in RPMI medium without supplements. RFL6 rat fibroblasts were maintained in Dulbecco modified Eagle medium (DMEM) with 10% FCS and PSG. Rat fibroblasts were infected with RCMV encoding green fluorescent protein (RCMV-GFP) (3) at a multiplicity of infection (MOI) of 1 and harvested 8, 24, 48, and 48 h in either TRIzol, for RNA analysis, or in Laemmli's sample buffer, for protein analysis.

To determine whether r129 is released from cells, we infected RFL6 cells with an MOI of 1. Uninfected cells were used as a negative control. At 24 h postinfection (hpi), the complete DMEM culture medium was replaced with DMEM without serum, and the cells were incubated for an additional 48 h. Then, cell-free and virus-free supernatants were produced by first pelleting cellular debris at 3,000 × *g* for 15 min. The virus was then removed by pelleting through a 20% sorbitol cushion by ultracentrifugation at 22,000 rpm for 1.25 h using a Beckman SW28 rotor. The clarified supernatants were subjected to a 10-fold concentration by ultrafiltration using Centricon Ultracel YM-30 filter devices (Millipore) following the manufacturer's instructions. The clarified supernatants from infected and uninfected cells were analyzed by Western blotting for the r129 protein as described below.

Adenovirus construction. Adenoviruses (Ad) expressing rat chemokine receptors CCR1, CCR2, CCR3, CCR4, CCR5, CCR6, CCR7, and CCR8 were constructed as previously described (21, 44, 51). Briefly, CCR gene fragments were PCR amplified from rat allograft heart cDNA using CCR-specific primers containing an N-terminal hemagglutinin (HA) tag. The amplified CCR genes were cloned into pAdTet7, which contains a Tet-responsive enhancer with a minimal CMV promoter and the simian virus 40 (SV40) poly(A) cassette portion of adenovirus E1A and a single LoxP site to increase recombination frequency. Recombinant adenoviruses were produced by cotransfection of 293 cells expressing Cre recombinase (Cre4 cells) with the plasmid pAdTet7-CCR and the adenovirus (Ad5-ψ5) genome containing the E1A/E3 deletion. This adenoviral backbone has a deletion of E1A/E3. Recombinant viruses were expanded on Cre4 cells, and we determined their titers by limiting dilution using 293 cells. CCR gene expression was driven by coinfection with Ad-Trans, which is an adenovirus that expresses a Tet-off transactivator (21, 44 51).

RCMV-r129ΔNT virus construction. We constructed a bacterial artificial chromosome (BAC) containing the RCMV-Maastricht strain genome called RCMV BAC. The BAC vector cassette was inserted into the RCMV genome at genes r144 to r146. The BAC cassette contains the chloramphenicol resistance marker and enhanced green fluorescent protein (eGFP) under the control of the HCMV major immediate early promoter and is flanked with LoxP sites in direct orientation. We used a modification of the standard two-step linear recombination protocol utilizing galactokinase (20) for positive and negative selection (53) coupled with kanamycin resistance (Kan^r)-negative selection to produce a seamless recombination scheme that will not interfere with the r129 ORF. The dual selection cassette containing both the galactokinase (20) gene and a kanamycin-resistance gene was generously provided by Dong Yu (Washington University, St. Louis, MO). In the first recombination step, recombinant bacteria (SW105) containing the RCMV BAC were transformed with a PCR product comprised of *galK*-Kan^r flanked by sequences homologous to regions flanking the r129 ORF in the RCMV genome. Recombinants were selected on LB agar containing kanamycin and verified via PCR of the r129 genomic region and sequencing for the presence of the *galK*-Kan^r cassette. In the second recombination step, the *galK*-Kan^r cassette was replaced with a PCR product with sequence homology to the recombination site containing the r129 ORF with the coding sequence for the first 10 amino acids deleted. Recombinants were selected on plates

containing 2-deoxy-galactose, a substrate toxic in the presence of *galK*, resulting in counterselection for BAC clones that have lost the *galK* marker and contain the desired mutation. Recombinants were verified via PCR of the r129 genomic region and sequencing for the mutation. The virus was reconstituted from RCMV BAC by electroporation of purified BAC DNA (Epicenter BaxMax kit) into RCMV-permissive fibroblasts.

RCMV infection of rats. All animals were housed in the Portland Veterans Administration Medical Center animal facility, which is accredited by the AAALAC and complies with the USDA and HHS requirements for animal care. F344 rats were purchased from Charles River Laboratories International (Wilmington, MA) and intraperitoneally (i.p.) infected with 1×10^5 PFU (55) of the Maastricht strain of RCMV (5, 6, 41). Tissues were harvested 3, 7, 14, 21, and 28 days postinfection (dpi). Tissue sections were treated for 24 h at 4°C with RNAlater (Qiagen, Valencia, CA) and then stored at −80°C without reagent until processing.

Heart transplantation. F344 rat donor hearts were transplanted heterotopically into Lewis recipients (26, 41). The recipient was intraperitoneally (i.p.) infected with 5×10^5 PFU (55) of either the RCMV BAC virus or RCMV-r129ΔNT 1 day postoperatively. The uninfected allograft recipient and native hearts from uninfected rats served as controls. Recipients received 10 mg/kg cyclosporine (CsA) (Novartis) intramuscularly per day for 10 days to prevent acute rejection. Animals were examined daily for overall health, and CR was determined by manual monitoring of heartbeat grade; upon graft failure, the hearts and other tissues were harvested (26). Paraffin-embedded tissue sections were stained with hematoxylin and eosin (H&E) and elastic van Gieson stain. The extent of neointimal formation (TVS) was determined by the neointimal index [NI = (intima area/lumen + intima area) × 100] (2, 41). The severity of allograft TVS and the time to rejection in recipients infected with RCMV BAC versus RCMV-r129ΔNT were compared to those in uninfected recipients using Student's *t* test. *P* values of <0.05 were considered statistically significant.

Quantitative RT-PCR detection of r129. Total RNA extracted using the TRIzol method (Life Technologies) from infected fibroblasts or tissues from infected rats was analyzed by quantitative reverse transcriptase PCR (RT-PCR) for the presence of r129 gene expression using the primers CGGACCTCAGAACGGACATAC (forward) and TCTCTGCAGGATAGTTGGATCTTG (reverse) and probe AATCTGACCAGACATGTATC. cDNA was generated using Superscript III (Invitrogen Life Technologies), analyzed using an ABI StepOne real-time PCR system, and normalized to L32 (41, 42). Gene amplicons served as quantification standards (sensitivity, ≤100 copies/gene). The r129 expression levels are depicted as relative copy numbers per microgram of total RNA.

Cloning and purification of recombinant r129-His proteins. The r129 open reading frame was cloned by making total RNA from RCMV-GFP-infected RFL6 cells 48 h postinfection (hpi) via a Qiagen RNeasy kit. The cDNA was made from total RNA using an Invitrogen Superscript III first-strand synthesis kit (18080-051). For bacterial expression and purification, r129 was amplified using primers designed to eliminate the r129 signal sequence (predicted using the SignalP 3.0 server) and to add a C-terminal 6×His tag. Truncation mutants were amplified similarly using primers to truncate the N-terminal 10 amino acids following the signal sequence cleavage site (r129-ΔNT) or the C-terminal 121 amino acids (r129-ΔCT). PCR products were cloned into a pGEM-T Easy (Promega) vector and subcloned into a pRSETB expression vector using NdeI and HindIII restriction sites. Point mutations (r129-C31A and -F43A) were made using 20-mer complementary primers that included the mutated sequence. Mutagenesis PCR was performed via a standard protocol using *Pfu* Turbo (Stratagene, Agilent Technologies, Santa Clara, CA) and transformation into TOP-10 competent *Escherichia coli* (Invitrogen). The pRSETB clones were confirmed via sequencing and transformed into Rosetta 2 competent *E. coli* (EMD4Biosciences 71405, Rockland, ME). For large-scale purification of r129-His proteins, Rosetta 2 competent *E. coli* were grown to an A_{600} of ~0.5 in 10 liters of 2× yeast extract and tryptone (YT) broth and induced with 0.5 M isopropyl-β-D-thiogalactopyranoside (IPTG) overnight at 30°C. Induced *E. coli* cells were pelleted at 7,000 rpm

for 10 min and lysed in 3 ml/g lysis buffer (300 mM NaCl, 50 mM NaPO$_4$, 20 mM Tris-HCl, 0.1 mM phenylmethylsulfonyl fluoride [PMSF], 3 mM 2-mercaptoethanol [2-ME] [pH 8.0]). Lysozyme (1 mg/ml) and DNase (5 μg/ml) were added and incubated for 10 min at room temperature (r.t.) followed by 30 min on ice. Cells were sonicated three times for 30 s each at 84 W. The inclusion bodies were pelleted from the cell sonicate at 10,000 rpm for 1 h at 4°C. Inclusion body extract (IBE) was made by resuspending pelleted inclusion bodies in binding buffer (300 mM NaCl, 50 mM NaPO$_4$, 20 mM Tris-HCl, 8 M urea, 3 mM 2-ME [pH 8.0]) and incubating for 30 min at 60°C. The IBE was applied to 1 ml equilibrated Talon metal affinity resin (catalog no. 63502; Clontech, Mountain View, CA) in a chromatography column. Resin was washed with 10 column volumes of wash buffer (300 mM NaCl, 50 mM NaPO$_4$, 20 mM Tris-HCl, 8 M urea, 3 mM 2-ME, 10% glycerol [pH 7.5]). Bound His proteins were eluted sequentially with one column volume each 0.1 M, 0.5 M, and 1 M imidazole in wash buffer. Eluted proteins were analyzed via SDS-PAGE and Coomassie staining and quantified by spectrophotometry. An S100 gel filtration column was equilibrated with gel filtration buffer (100 mM Tris-HCl, 8 M urea, 3 mM 2-ME [pH 8.0]) using an Akta fast-performance liquid chromatograph (GE Lifesciences). Approximately 8 to 15 mg of purified His-tagged protein was loaded onto the column, and 0.5-ml fractions were collected and analyzed via SDS-PAGE and Coomassie staining. Peak protein fractions were pooled and dialyzed sequentially against 6 M, 4 M, 2 M, 1 M, 0.5 M, and 0.1 M urea in 20 mM Tris-HCl with a final dialysis into 20 mM Tris-HCl. Insoluble or misfolded proteins were removed via centrifugation at 10,000 rpm for 1 h. Soluble protein was quantified via spectrophotometry and dialyzed into 1% acetic acid and finally into 0.1% trifluoroacetic acid (TFA). Aliquots of r129 (20 μg each) were lyophilized and stored at −80°C. For chemotaxis assays, the His-tagged proteins were reconstituted in PBS and stored at a 10 μg/ml working concentration at −80°C.

In vitro migration assays. NR8383 macrophages or primary lymphocytes (derived from peripheral blood, bone marrow, or spleen) were suspended in RPMI medium without supplements at 2×10^6 cells/ml. Approximately 100 μl (2×10^5 cells) was added to the top well of a chemotaxis chamber (96-well Millipore multiscreen, 3.0-μm pore size). The r129-His protein or a control recombinant protein in RPMI medium without supplements or medium alone was added to the bottom chamber as a chemotactic stimulus. Recombinant rat MCP-1 was used as a positive control for migration assays (catalog no. 3144-JE; R&D Systems). Chemotaxis was allowed to proceed for 1 h at 37°C. The top chambers were discarded, and migrated cells in the bottom chamber were quantified via fluorescence using CyQuant (Invitrogen, Life Technologies) and read on a Molecular Devices Flexstation II fluorescence plate reader. Migration was determined from 4 to 6 independent wells per assay per condition. The means and standard deviations were calculated. The percentages of control values were generated by comparing chemokine-stimulated cells to unstimulated medium-only control cells, and the results were analyzed using Student's *t* test. *P* values of <0.05 were considered statistically significant.

Fluorescence-accelerated cell sorting. Splenocytes were isolated as described and resuspended at 1×10^8 cells/ml in 10 ml of PBS plus 1% FBS. Antibodies, antigen-presenting cell (APC)-conjugated mouse anti-rat CD3 antibody (1F4), APC-conjugated mouse anti-rat CD4 (OX-35), biotin-conjugated mouse anti-rat CD8α (OX-8), phosphatidylethanolamine (PE)-conjugated hamster anti-rat CD62L (HRL1) (BD Pharmingen), and fluorescein isothiocyanate (FITC)-conjugated mouse anti-rat CD45R (His24) (eBioscience) were added and incubated at 4°C for 40 min. Cells were washed 2 times with PBS plus 1% FBS, and streptavidin-FITC secondary antibody was applied at 1 μg/1×10^8 cells for 30 min at 4°C followed by washing as done before. Stained cells were resuspended at 5×10^7 cells/ml in PBS + 1% FBS and sorted on a BD FACSAria II cell sorter. Sorted populations were centrifuged for 5 min at 2,000 rpm and resuspended at 2×10^6/ml in RPMI medium without supplements. Chemotaxis assays were performed and analyzed as described above on B cells
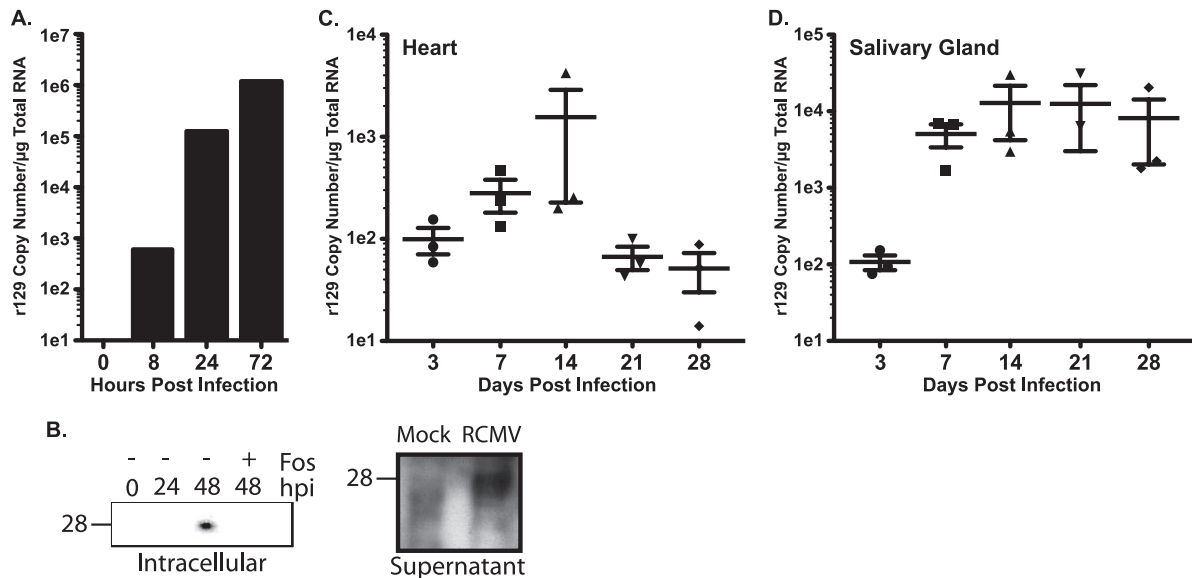
FIG 1 (A, C, and D) RCMV r129 is expressed with late viral expression kinetics. RCMV r129 mRNA was detected by quantitative RT-PCR using a gene-specific primer and probe set. RCMV-infected fibroblasts were harvested at 0 (mock infected), 8, 24, and 72 hpi. RCMV r129 mRNA was quantified by qRT-PCR in heart and salivary gland tissues from infected rats at 3, 7, 14, 21, and 28 days postinfection ($n = 3$ individual rats). (B) r129 protein was detected in culture supernatants and cellular lysates from RCMV-infected cells by immunoblotting using r129-specific antisera. Cells were treated with foscarnet (25 μg/ml) for 48 h to differentiate between early and late viral gene expression. Clarified supernatants were concentrated 10-fold and analyzed by Western blotting for r129.

($CD3^-CD45R^+$), T cells ($CD3^+CD45^-$), non-B/non-T ($CD3^-CD45^-$), CD4-EM ($CD4^+CD62L^{lo}$), CD4-naïve/CM ($CD4^+CD62L^{hi}$), CD8-EM ($CD8^+CD62L^{lo}$), or CD8-naïve/CM ($CD8^+CD62L^{hi}$) cells.

Generation of mouse polyclonal anti-r129 antibody. BALB/c mice were subjected to peritoneal injection twice, 21 days apart, with 20 μg of r129-His emulsified with the Sigma adjuvant system (catalog no. S6322-1VL; Sigma). Two weeks after the second injection, the mice were bled, and the titer of anti-r129 was determined by enzyme-linked immunosorbent assay (ELISA). Terminal bleeds were then prepared from the mice that responded best.

Western blot analysis. RCMV-infected cells were lysed in 2× Laemmli's sample buffer, and 20 μl was loaded onto NuPAGE 4 to 12% bis-Tris gradient gels (Invitrogen, Life Technologies) and run in morpholineethanesulfonic acid (MES) buffer. Similarly, 10 μl of 10-fold-concentrated supernatants from infected and uninfected cells was mixed with a similar volume of 2× sample buffer and subjected to SDS-PAGE. Proteins were transferred to Immobilon-P blotting membranes and dried overnight. The membranes were blocked in 2% milk plus 0.02% Tween 20 (Block) for 15 min at r.t. Primary mouse polyclonal α-r129 antibodies were added at a 1:1,000 dilution in Block for 1 h at r.t., and the membranes were washed for 10 min in Tris-buffered saline (TBS) plus 0.2% Tween (TBST). Secondary goat anti-mouse-horseradish peroxidase (HRP) conjugate was added at a 1:40,000 dilution in Block for 20 min at r.t., and the membranes were washed three times for 10 min each in TBST. The membranes were exposed to ECL Advance Lumigen-TMA (GE Healthcare) for 1 min and exposed to BioMax light film (Kodak).

r129 labeling and ligand-binding assay. Wild-type (WT) r129 (20 μg) was labeled with an infrared dye (IRDye 800CW) using the Microscale labeling kit by Li-Cor Biosciences. The infrared labeling dye was dissolved in purified water, and 1.6 μl was incubated with 20 μg of r129 protein for 2 h at 20°C. A Zeba spin desalting column (Pierce-Thermo Scientific) was used to remove the unbound dye by performing the desalting procedure. Aliquots of the labeled r129 protein (IRDye 800CW r129) were frozen at −80°C until used. For the ligand-binding assay, Vero cells were grown to 90% confluence in 96-well plates. The cells were infected with Ad-CCR and/or Ad-Trans. At 18 h postinfection the cells were washed and incu-

bated with 0.5 μg/ml of IRDye 800CW r129 for 2 min at room temperature in at least triplicate wells. For competitive binding assays, cells were treated with 0.5 μg/ml of IRDye 800CW r129 mixed with 1 μg/ml of unlabeled WT r129 protein. After 2 min, the cells were fixed with 4% paraformaldehyde for 15 min at room temperature and washed 3 times with 200 μl of PBS. The plate was scanned using a Li-Cor Odyssey infrared imaging system. The cells infected with Ad-Trans only were used as a negative control, and quantifications of fold increase in binding activity were determined by comparing the fluorescence intensity to this negative control.

RESULTS

RCMV r129 is expressed with late viral gene kinetics. The expression and function of the CMV-encoded chemokines are relatively unknown. Therefore, in order to characterize r129 *in vitro* and *in vivo*, we first determined r129 gene expression by quantitative reverse transcriptase PCR (qRT-PCR). r129 gene expression was detected in RCMV-infected rat fibroblasts by 24 h postinfection (hpi), and the expression was maximal by 72 hpi (Fig. 1A), suggesting that r129 is expressed with either early or late viral gene expression kinetics. In order to gain further insight into the expression of r129 during RCMV infection, we produced a mouse polyclonal serum directed against recombinant r129-His. To determine r129 protein expression kinetics, rat fibroblasts were infected with RCMV at an MOI of 1, and cellular lysates were harvested at 8 hpi (immediate early [IE] viral kinetics) and 48 hpi (late viral kinetics). An additional infected sample was treated with 0.5 mM foscarnet to block late gene expression and harvested at 48 hpi (early viral kinetics). Lysates were analyzed by SDS-PAGE and Western blotting utilizing our anti-r129 polyclonal mouse serum (Fig. 1B). We detected r129 expression at 48 hpi, and protein expression of r129 is sensitive to foscarnet, suggesting that the gene is expressed with late viral expression kinetics. Importantly, we also detected r129 protein in clarified supernatants produced

A.
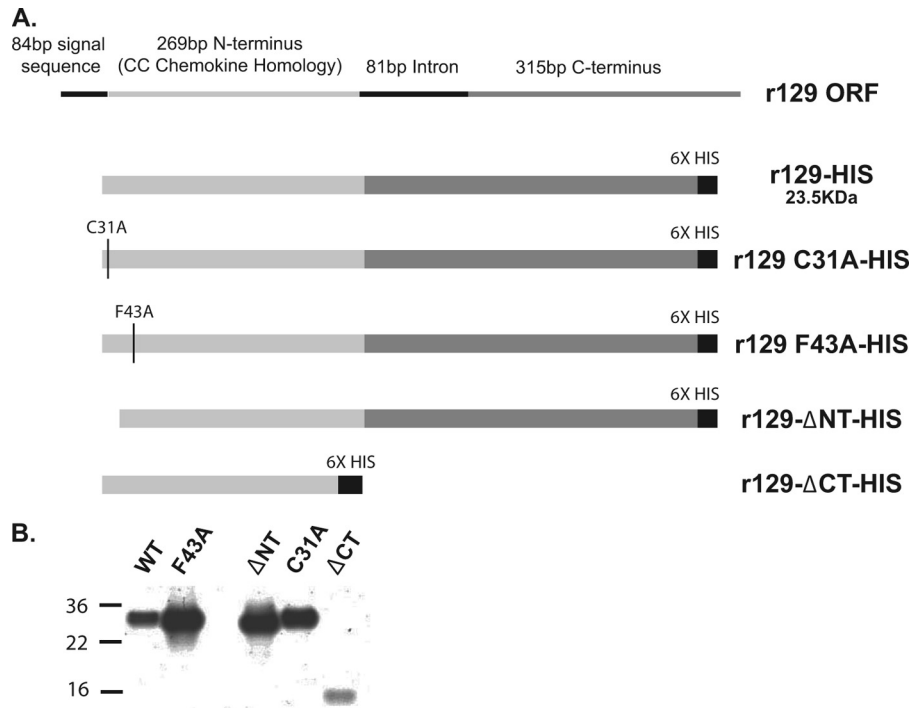
FIG 2 Schematic of RCMV r129 gene and mutants. (A) Schematic representation of the r129 gene and recombinant r129-His protein and mutants produced for this study. (B) r129-His protein and mutants expressed in *E. coli* and refolded as described in Materials and Methods. Recombinant r129-His proteins were analyzed by SDS-PAGE, and the gel was stained with Coomassie brilliant blue.

from infected cells but not uninfected cells, indicating that r129 protein is released from infected cells. Next, we determined whether r129 is expressed during *in vivo* infection of rats by quantifying r129 gene expression at various times postinfection in heart and salivary glands. Interestingly, r129 mRNA is expressed in heart tissues from infected rats at 7 and 14 days postinfection (dpi) (Fig. 1C) and in the salivary glands at 7, 14, 21, and 28 dpi (Fig. 1D). While expression levels were relatively higher in the salivary glands, this potentially reflects the known limited number of infected cells in the heart compared to those in the salivary glands (45).

Recombinant r129 protein is chemotactic. The protein encoded by r129 contains an N-terminal signal peptide sequence, a C-C motif, and a chemokine fold, as well as a large C-terminal domain that in comparative analyses does not map to any other known protein motif (Fig. 2A). In addition, we determined above that the r129 protein is released from infected cells. Thus, to determine whether the r129 open reading frame encodes a functional CC chemokine and to characterize its functional domains, we generated recombinant wild-type r129 protein as well as four r129 mutants (r129-ΔNT, -ΔCT, -C31A, and -F43A) based on structure/function studies of other CC chemokines (15, 54). These recombinant proteins contained a C-terminal 6×His tag for purification, and the proteins were refolded by standard procedures (14). The final protein products are depicted in Fig. 2B. We performed *in vitro* migration assays in a 96-well transwell format by seeding an NR8383 rat macrophage cell line or primary rat PBMC in the upper chamber in serum-free medium. Then, various concentrations of r129-His or commercial recombinant rat MCP-1 chemoattractants were added to the wells below. After a 1-h incubation, the migratory cells present

in the bottom chamber were quantified using the fluorescent stain CyQuant. We found that r129-His is chemotactic to both NR8383 macrophages (Fig. 3A) and PBMC (Fig. 3B) at the same working concentration range as recombinant MCP-1. The peak migratory activity for both chemokines was observed at 10^{-9} to 10^{-10} g/ml (Fig. 3), which is the effective concentration range for most chemokines.

Having established that r129 is a functional chemokine, we next identified r129 domains that contribute to chemotactic activity using the mutant r129 proteins shown in Fig. 2. We tested the ability of each mutant r129 protein to induce chemotaxis using NR8383 rat macrophage cells as well as primary rat lymphocytes isolated from PBMC, bone marrow, and spleen (Fig. 4). As expected, deletion of the N-terminal 10 amino acids of r129 completely abrogated the chemotactic activity of the molecule for all cell types used in this assay. Similarly, mutation C31A, which comprises the first of the two sequential cysteines in the CC motif, resulted in a nonfunctional r129 molecule. Deletion of the C terminus of r129 had no effect on chemotactic activity. Interestingly, the r129-F43A mutant displayed a differential migration phenotype depending on the source of the lymphocytes used in the assay. While r129-F43A was not chemotactic to NR8383 rat macrophages, this mutant protein mediated migration of PBMC similar to that observed with r129-WT-treated cells (Fig. 4A and B). Lymphocytes isolated from rat bone marrow and rat spleen displayed an intermediate phenotype when stimulated with r129-F43A (Fig. 4C and D). These results suggest that mutation of F43 results in altered receptor binding, but whether this is due to a decrease in receptor affinity or a receptor type switch remains to be determined.

To determine whether the nonfunctional r129 mutants inhibit
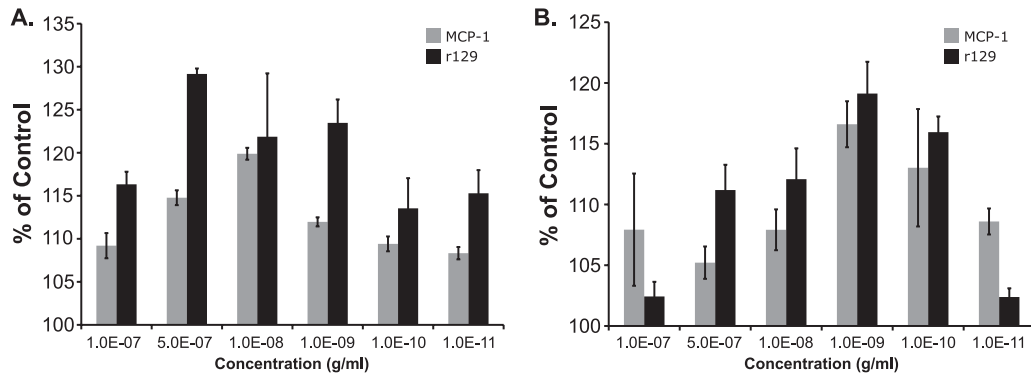
FIG 3 The RCMV r129 protein induces cellular migration. Transwell migration assays were performed with either a rat macrophage cell line (A) or primary rat peripheral blood lymphocytes (B) using various concentrations of the RCMV-r129 protein (black bars) or rat MCP-1 (gray bars). The migration index was compared to that of the untreated control cells and expressed as a percentage of the control ($n = 10$).

the migratory action of r129-WT, we performed competition assays using NR8383 rat macrophages in which cells were simultaneously stimulated with r129-WT and various concentrations of the r129 mutants. Interestingly, r129-ΔNT, r129-C31A, and r129-F43A were able to competitively inhibit the migration of NR8383 stimulated with r129-WT (Fig. 5). The mutant r129-C31A was the most potent inhibitor, as 1 ng/ml was sufficient to competitively

inhibit the promigratory signaling of a 10-ng/ml r129-WT stimulus (Fig. 5B). The r129-ΔNT and r129-F43A proteins were inhibitory at concentrations equal to or higher than the amount of r129-WT used in the assay (Fig. 5A and C).

r129 recruits CD62L^lo CD4^+ T cells. We demonstrated that r129 protein stimulates chemotaxis of primary lymphocytes isolated from the spleen, blood, or bone marrow. However, the iden-
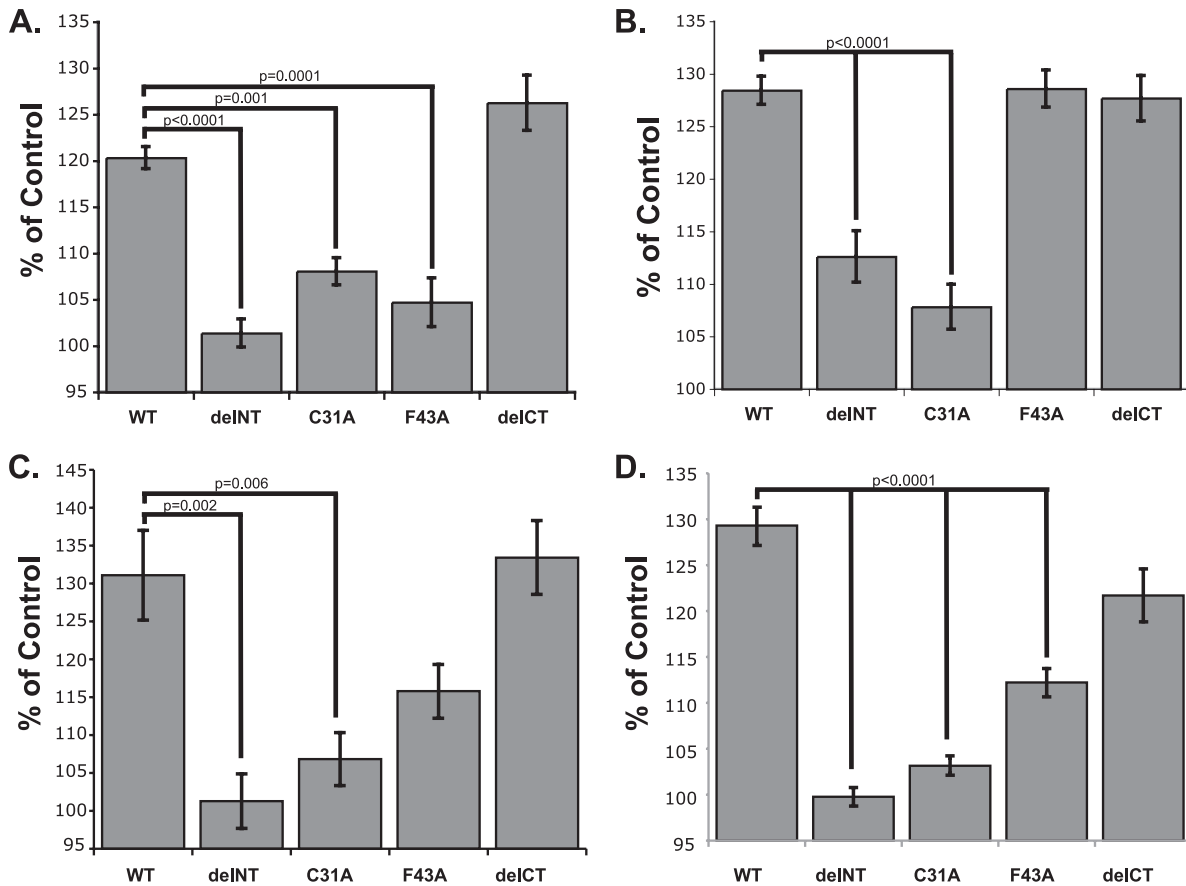
FIG 4 *In vitro* migration of r129 mutants. Transwell migration assays were performed using rat alveolar macrophages (A), primary rat PBMC (B), primary rat splenocytes (C), and primary rat bone marrow lymphocytes (D) stimulated with 0.1 ng/ml of r129-His-WT, -delNT, -C31A, -F43A, or -delCT. For panels A and B the total *n* is 14, and for panels C and D the total *n* is 10. The migration index was compared to that of the untreated control cells and expressed as a percentage of the control. *P* values were determined by Student's *t* test using Excel.
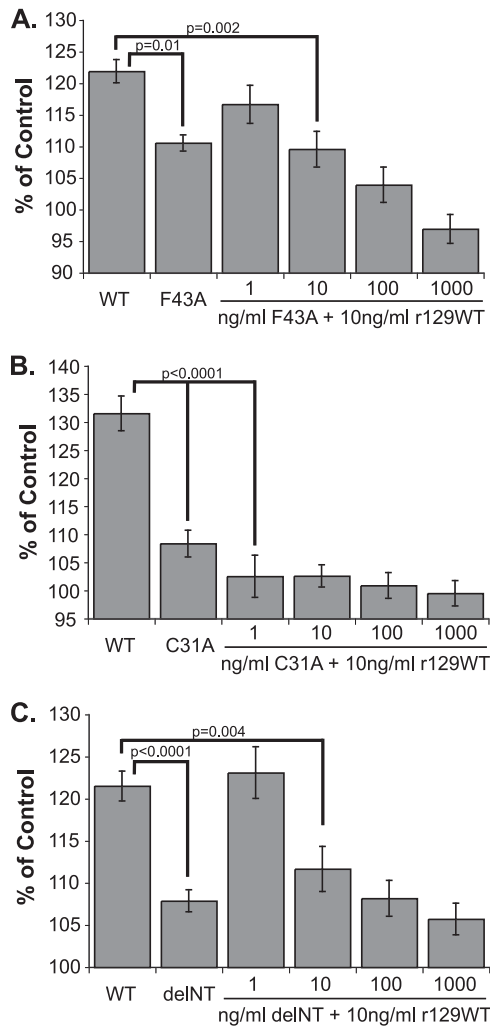
**FIG 5** RCMV r129 mutants compete with r129-WT chemotactic stimulus. Shown are the results of transwell migration assays using rat macrophage cells stimulated with 10 mg/ml WT r129 protein and/or increasing concentrations of the mutant proteins F43A (A), C31A (B), and ΔNT (C). The migration index was compared to that of the untreated control cells and expressed as a percentage of the control. *P* values were determined by Student's *t* test using Excel.

FIG 6 RCMV r129 induces the migration of T cells. Primary splenocytes were subfractionated into T cell, B cell, and non-T cell and non-B cell populations using antibodies directed against CD3 and CD45R. Results of the analyses of the sorted cells are depicted in panel A. Transwell migration assays using the isolated cells were stimulated with 10 mg/ml WT r129 protein (gray bars) or the mutant r129-ΔNT (black bars). The migration index was compared to that of the untreated control cells and expressed as a percentage of the control. *P* values were determined by Student's *t* test using Excel.

tities of these migrating lymphocytes were unknown. To determine the lymphocyte cell types targeted by the r129 protein, we performed *in vitro* migration assays using lymphocyte subpopulations isolated by fluorescence-activated cell sorting (FACS). In the first experiment, we sorted three populations from splenocytes for *in vitro* migration assays: (i) CD3+ CD45R− (T cells), (ii) CD3− CD45R+ (B cells), and (iii) CD3− CD45R− (non-B/non-T cells), as depicted in Fig. 6A. We found that T cells preferentially migrated in response to r129 (Fig. 6B), while the B cell population and non-B/non-T cell populations failed to migrate much above background levels. As expected, none of the cells migrated in response to treatment with the mutant protein r129-ΔNT. To identify the r129-responding T cell subset(s), we performed a second experiment in which splenocytes were stained for CD4, CD8, and the maturation marker CD62L. CD62L is highly expressed on naïve (Na) and central memory (CM) T cells and is less prevalent on effector memory (EM) T cells. In this experiment we

sorted four populations for *in vitro* migration: (i) CD4+ CD62L^hi (CD4 Na/CM), (ii) CD4+ CD62L^lo (CD4 EM), (iii) CD8+ CD62L^hi (CD8 Na/CM), and (iv) CD8+ CD62L^lo (CD8 EM). Results of the analysis of the sorted T cells are depicted in Fig. 7A. This experiment revealed that only the CD4 Na/CM population migrated in response to an r129 chemotactic gradient (Fig. 7B). Taken together, these results indicate that r129 contains potent chemokine activity and is able to recruit macrophages and CD62L^hi CD4+ T cells.
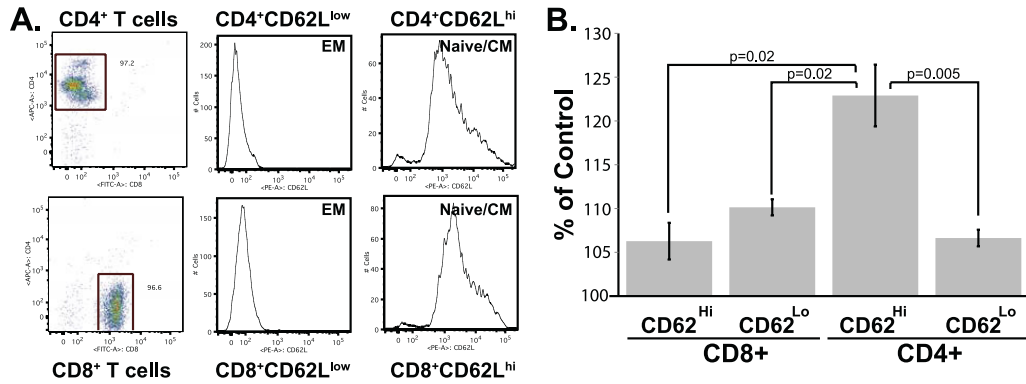
FIG 7 RCMV r129 induces the migration of CM/naïve CD4 T cells. Primary splenocytes were subfractionated into separate T cell populations using antibodies directed against CD4, CD8, and the activation marker CD62L. Results of the analyses of the sorted T cells are depicted in panel A. Transwell migration assays using the isolated cells were stimulated with 10 mg/ml WT r129 protein. The migration index was compared to that of the untreated control cells and expressed as a percentage of the control. P values were determined by Student's *t* test using Excel.

The r129 binds multiple CC chemokine receptors. Next we sought to identify the cellular CC chemokine receptors to which r129 binds using a ligand-binding assay. We constructed adenovirus vectors expressing rat CCR1, CCR2, CCR3, CCR4, CCR5, CCR6, CCR7, and CCR8 as previously described (21, 44, 46, 51). For the ligand-binding assay we labeled WT r129 protein with an infrared dye (IRDye 800CW; LiCor Biosciences). The binding of IRDye 800CW r129 to intact Vero cells expressing rat chemokine receptors was quantified in a 96-well microplate assay. Confluent monolayers of Vero cells were transduced with Ad-Trans alone (negative control) or with individual Ad-rat CCRs. At 18 h postinfection, the cells were washed, incubated with IRDye 800CW r129 (0.5 μg/well), and then fixed (16). After fixation the cells were washed, and the plate was scanned using a Li-Cor Odyssey infrared imaging instrument. The binding data are represented as the fold increase in fluorescence over that of the trans-only control. IRDye 800CW r129 consistently binds to cells expressing CCR3,

CCR4, CCR5, and CCR7, which is blocked treatment with unlabeled ligand, indicating that the interaction is specific for a subset of CC chemokine receptors (Fig. 8).

RCMV-accelerated TVS and CR is dependent upon r129. In order to determine whether RCMV r129 is required for RCMV-induced acceleration of TVS, we constructed the mutant virus RCMV-r129ΔNT by replacing the WT r129 sequence in the bacterial artificial chromosome containing the Maastricht strain of RCMV (RCMV-BAC) with a version containing the N-terminal 10-amino-acid deletion that we described above. The WT and mutant BAC DNAs were purified and transfected into rat fibroblasts in order to reconstitute the virus. The mutant virus grows to wild-type levels in fibroblasts and displays a higher infectious particle-per-genome level than WT RCMV and expresses the mutant version of r129 protein (Fig. 9). We performed heart transplants using the F344/Lewis rat model as previously described (25, 26, 41–43) and infected allograft recipients with the r129ΔNT mutant
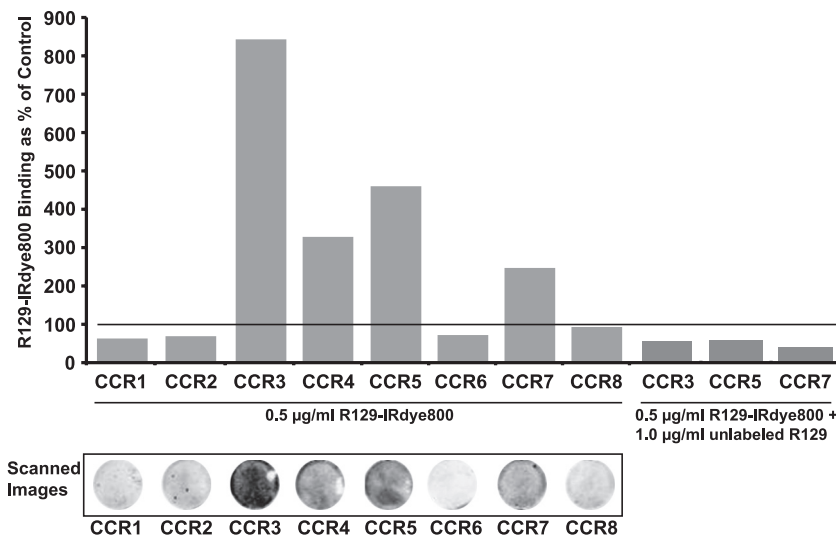
FIG 8 RCMV r129 binds rat CC chemokine receptors. Vero cells were plated in 96-well plates and infected with adenoviruses expressing rat CC chemokine receptors. r129 was conjugated to IRDye 800CW, and 0.5 μg/ml of the ligand was added to Vero cells expressing rat cellular chemokine receptors for 2 min at room temperature. Competition assays were performed by incubating cells with 0.5 μg/ml of labeled ligand with 1.0 μg/ml of unlabeled r129. The cells were washed and fixed, and then the plate was scanned using a Li-Cor infrared imaging system (representative scanned images are shown). Binding was determined as a percentage of the control cells lacking expression of rat chemokine receptors. Data are a representation of 5 individual experiments.
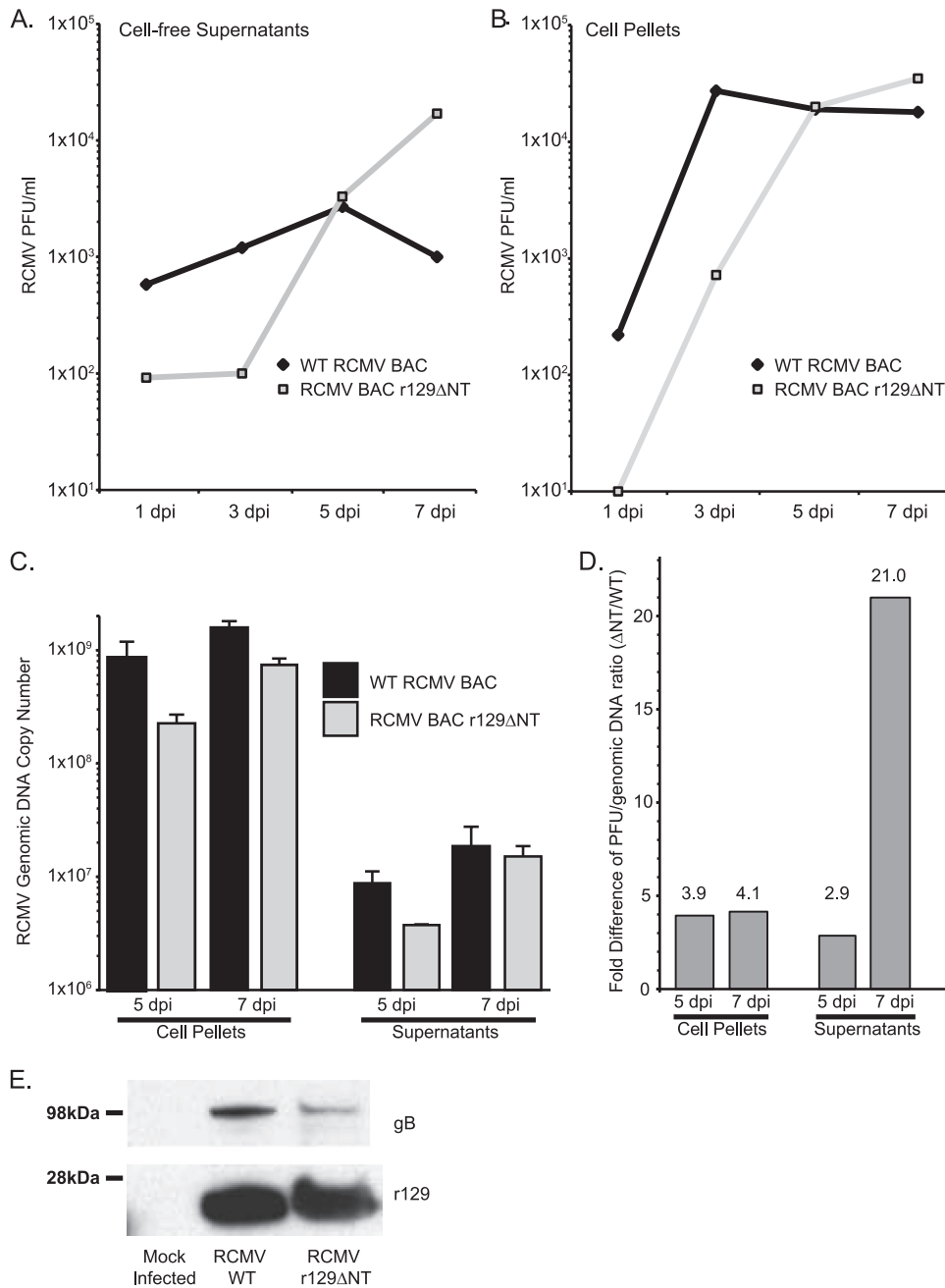
FIG 9 Characterization of RCMV-r129ΔNT. Rat fibroblasts were infected with RCMV-BAC or RCMV-BACr129ΔNT at a multiplicity of infection equal to 0.5. (A to C) At 1, 3, 5, and 7 days postinfection, the supernatants and cell pellets were collected, virus levels were determined by titration (A and B), and the viral DNA genome was quantified by real-time PCR (C). (D) Viral PFU per genomic DNA ratio were calculated, and the fold differences between the RCMV-BAC and RCMV-BACr129ΔNT were calculated and displayed graphically. Cellular lysates were also analyzed by Western blotting by staining with antibodies directed against RCMV-gB or r129. Uninfected cells were used as a negative control.

virus (5×10^5 PFU), and we compared the time to rejection and the severity of TVS to those of the recipients infected with RCMV-BAC (5×10^5 PFU) and uninfected controls. The time to rejection was significantly longer in the RCMV-r129ΔNT recipients (100 ± 0 days, study endpoint) than that inseen in the RCMV-BAC-infected recipients (46.25 ± 2.8 days) ($P < 0.0001$) (Fig. 10A). The uninfected controls paralleled the RCMV-r129ΔNT recipients, rejecting at 100 ± 3.1 days. The severity of TVS was also signifi-

cantly less in the RCMV-r129ΔNT allografts than in the RCMV-BAC allografts (NI = 57.5 ± 6.8 versus 83 ± 8; $P = 0.021$) (Fig. 10A). Again, the severity of TVS in uninfected control allografts paralleled that of the RCMV-r129ΔNT (NI = 56 ± 2.8). Furthermore, the allografts from recipients infected with RCMV-r129ΔNT grossly showed less inflammatory cellular infiltrate on H&E evaluation (Fig. 10B) than did either the RCMV-BAC allografts or the uninfected allografts, supporting role for r129 in cellular migration.
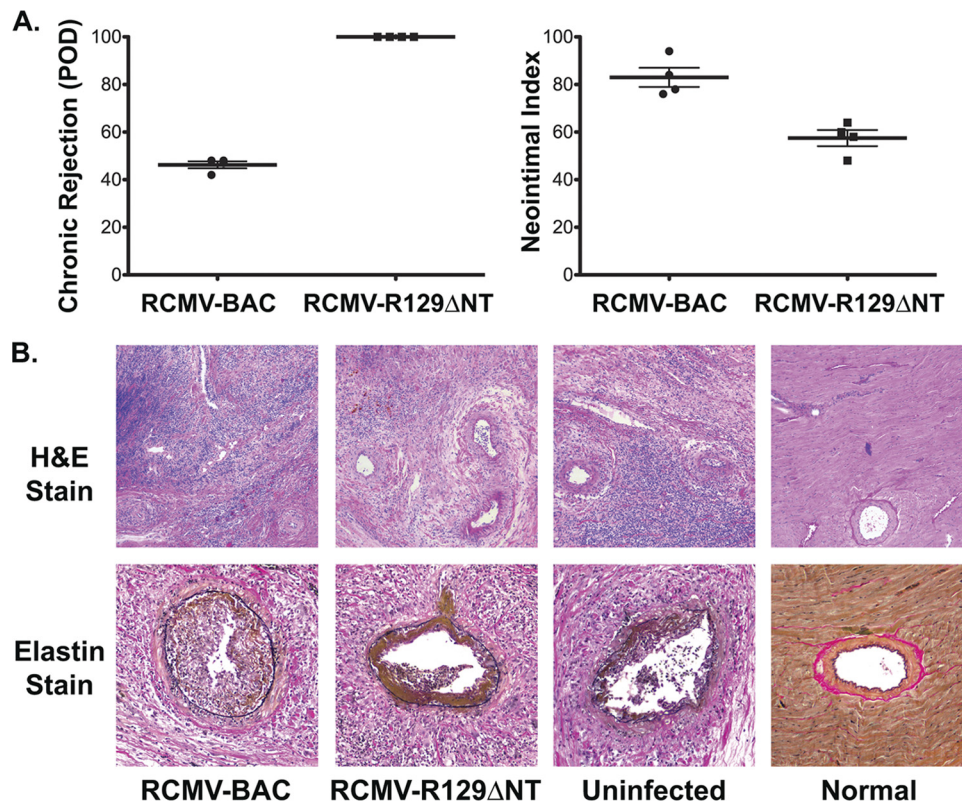
FIG 10 RCMV-r129ΔNT fails to accelerate rat heart chronic rejection and TVS. F344 rat donor hearts were transplanted into naïve Lewis recipients. The rats were treated with CsA for 10 days to prevent acute rejection. The recipient rats were infected 1 day posttransplantation with 5×10^5 PFU of RCMV (RCMV-r129ΔNT or RCMV-BAC). A third group remained uninfected as a negative control. (A) The time to rejection was determined by palpating the heart for induration of heartbeat. The level of vascular disease (TVS) was determined by (B) Histological representative of rat heart vessels is shown for the RCMV-r129ΔNT, RCMV-BAC, and uninfected control groups. The presence of cellular immune infiltrates was detected by H&E staining. Vascular disease was detected by elastin staining.

DISCUSSION

Herpesviruses, including the cytomegaloviruses, encode chemokines and chemokine receptors. However, the roles of these genes in virus infection and their effects on pathogenesis remain unclear. Rat cytomegalovirus encodes two potential chemokine receptors (r33 and r78) and two chemokine ligands (r129 and r131). All of these genes have homologues present in HCMV. In our current study, we sought to characterize RCMV-r129, a homologue of HCMV-UL128. We found that r129 is expressed with late viral kinetics during infection of cultured fibroblasts and that the protein is released into the culture supernatants. In addition, r129 is expressed in heart tissues and detectable at 7 and 14 days postinfection and in the salivary glands from 7 dpi to at least 28 dpi. This finding suggests that r129 is involved in viral persistence and may manipulate the host during *in vivo* infections. Thus, we sought to determine whether r129 is a functional chemokine. Utilizing recombinant proteins we have discovered that r129 induces the cellular migration of macrophages and naïve/central memory $CD4^+$ T cells. We have also identified key motifs in the r129 protein that have important functional roles in migration. Furthermore, we showed that r129 binds to CCR3, CCR4, CCR5, and CCR7, supporting the concept that this is a functional chemokine. These chemokine receptors are specifically involved in recruiting macrophages and T cells to the sites of inflammation and allograft rejection. Our findings support the premise that CMV may en-

code chemokines that induce the migration of susceptible cells in order to propagate and disseminate the viral infection (33, 34). Additionally, these chemokines may promote immune cell migration in order to create a proinflammatory environment, which would ensure continual virus replication leading to viral persistence. CMV-encoded chemokines also function to promote allograft rejection. We have shown in our *in vivo* transplant studies with a mutated virus that r129 is necessary for CMV-accelerated TVS, further confirming its role in chronic transplant rejection.

Numerous structure/activity studies have elucidated the sequence determinants of chemokine receptor binding and activity (17, 35). chemokines contain multiple conserved regions that are coordinately involved in ligand binding, including the N-terminal loop (N-loop), the 30s loop, residues directly adjacent to the disulfides, and specific residues in the α-helix. These regions also dictate receptor-binding specificity, and as such, natural heterogeneity exists in the amino acid residues that make up these motifs. However, there are also specific amino acids including the conserved Cys residues that are required for chemokine structure and ultimately function. As expected, the mutation of one of the conserved Cys residues of the CC motif present in the N-loop of r129 prevented chemotactic activity of the chemokine and produced a chemokine that inhibited migration induced by the WT ligand. Deletion of the large C-terminal region of r129 had no effect on migration, suggesting that this region is not involved in

ligand binding and may have additional yet-undetermined function. The F43 residue of r129 is positioned as the end amino acid residue of the N-loop, which is part of the putative chemokine receptor-binding domain that confers binding specificity. Interestingly, mutation of the F43 residue resulted in a ligand that induced migration of primary rat PBMC but not rat macrophages, suggesting that this ligand has differential binding specificity compared to that of the WT protein. It would be interesting in future experiments to determine whether F34A-r129 has a different chemokine receptor-binding profile and to dissect what role this specificity plays in viral pathogenesis and during CMV-accelerated transplant rejection.

Our observation that the r129 protein is a functional chemotactic cytokine has significant implications for the RCMV-mediated development of transplant vascular disease (TVS) and chronic allograft rejection. Mechanisms of vascular disease and chronic rejection in solid organ transplants have long been thought to be a result of chronic inflammation. We have recently shown significant recruitment of T cells into RCMV-infected allografted hearts in our rat model of chronic rejection (41). Importantly, when donor animals are latently infected with RCMV, the chronic rejection phenotype is insensitive to ganciclovir treatment, suggesting that RCMV infection primes the inflammatory process in these organs and active CMV replication is not necessary to drive CR posttransplantation (25). Latently infected hearts contain large accumulations of T cells and macrophages prior to transplantation. We hypothesize that r129-mediated recruitment of immature T cells and macrophages into the heart prior to transplantation may contribute to the proinflammatory conditioning of the organ. CMV is also associated with the development of other vascular diseases, such as atherosclerosis and restenosis following angioplasty. Mechanistically, how CMV promotes vascular disease is still unclear. However, there are multitudes of data demonstrating that the attraction of macrophages/myeloid lineage cells and T cells is more prevalent during CMV infection. Importantly, Vliegen et al. demonstrated in a model of atherosclerosis that MCMV-infected ApoE$^{-/-}$ mice have increased infiltration of T cells in the arterial wall compared to that in uninfected controls and that the infected mice have a correspondingly higher level of gamma interferon (IFN-γ) (48, 50), which promotes macrophage differentiation (36, 37, 49). IFN-γ is a potent activator of CMV in macrophages, and its upregulation promotes increased virus replication (13, 36–39).

Both RCMV-r129 and HCMV-UL128 share significant homology, including the CC chemokine motif. Recently, the UL128 protein was reported to reduce expression of CCR1, CCR5, and CCR2 and blocked the migration of human macrophages (40). However, it may be that, because the recombinant UL128 protein contained an N-terminal epitope tag and a His tag, adding additional amino acids to the functional end of the chemokine (40), the protein was inactive. The addition of amino acids to the N terminus typically inactivates chemotactic activity of the ligands. Similarly, deletion of the N-terminal amino acids results in defective cellular migration. Furthermore, we have demonstrated that r129ΔNT specifically failed to promote migration, and infection of allograft recipients with RCMV-r129ΔNT did not accelerate TVS. These findings indicate that r129 plays an important role in mediating vascular disease and chronic allograft rejection. Future studies are planned to further characterize the role of viral chemo-kines in pathogenesis, in immune evasion, and in the development of chronic transplant rejection and vascular diseases.

REFERENCES

1. **Akter P, et al.** 2003. Two novel spliced genes in human cytomegalovirus. J. Gen. Virol. **84**:1117–1122.
2. **Armstrong AT, Strauch AR, Starling RC, Sedmak DD, Orosz CG.** 1997. Morphometric analysis of neointimal formation in murine cardiac allografts. Transplantation **63**:941–947.
3. **Baca Jones CC, et al.** 2009. Rat cytomegalovirus infection depletes MHC II in bone marrow derived dendritic cells. Virology **388**:78–90.
4. **Boomker JM, de Leij LF, The TH, Harmsen MC.** 2005. Viral chemokine-modulatory proteins: tools and targets. Cytokine Growth Factor Rev. **16**:91–103.
5. **Bruggeman CA, Meijer H, Bosman F, van Boven CP.** 1985. Biology of rat cytomegalovirus infection. Intervirology **24**:1–9.
6. **Bruggeman CA, Schellekens H, Grauls G, Debie WM, van Boven CP.** 1983. Rat cytomegalovirus: induction of and sensitivity to interferon. Antiviral Res. **3**:315–324.
7. **Bruning JH.** 1994. Enhancement of transplantation associated atherosclerosis by CMV, which can be prevented by antiviral therapy in the form of HPMPC. Transpl. Int. **7**(Suppl. 1):S365–S370.
8. **Capers Q, IV, et al.** 1997. Monocyte chemoattractant protein-1 expression in aortic tissues of hypertensive rats. Hypertension **30**:1397–1402.
9. **Cha TA, et al.** 1996. Human cytomegalovirus clinical isolates carry at least 19 genes not found in laboratory strains. J. Virol. **70**:78–83.
10. **Fleming P, et al.** 1999. The murine cytomegalovirus chemokine homolog, m131/129, is a determinant of viral pathogenicity. J. Virol. **73**:6800–6809.
11. **Gao W, et al.** 2001. Beneficial effects of targeting CCR5 in allograft recipients. Transplantation **72**:1199–1205.
12. **Gao W, et al.** 2000. Targeting of the chemokine receptor CCR1 suppresses development of acute and chronic cardiac allograft rejection. J. Clin. Invest. **105**:35–44.
13. **Hahn G, Jores R, Mocarski ES.** 1998. Cytomegalovirus remains latent in a common precursor of dendritic and myeloid cells. Proc. Natl. Acad. Sci. U. S. A. **95**:3937–3942.
14. **Jones JM, Messauodi I, Estep RD, Orzechowska B, Wong SW.** 2008. Monkeypox virus viral chemokine inhibitor (MPV vCCI), a potent inhibitor of rhesus macrophage inflammatory protein-1. Cytokine **43**:220–228.
15. **Kaptein SJ, et al.** 2004. The r131 gene of rat cytomegalovirus encodes a proinflammatory CC chemokine homolog which is essential for the production of infectious virus in the salivary glands. Virus Genes **29**:43–61.
16. **Kovar JL, Volcheck WM, Chen J, Simpson MA.** 2007. Purification method directly influences effectiveness of an epidermal growth factor-coupled targeting agent for noninvasive tumor detection in mice. Anal. Biochem. **361**:47–54.
17. **Kuloglu ES, et al.** 2001. Monomeric solution structure of the prototypical 'C' chemokine lymphotactin. Biochemistry **40**:12486–12496.
18. **Lemstrom K, et al.** 1995. Cytomegalovirus antigen expression, endothelial cell proliferation, and intimal thickening in rat cardiac allografts after cytomegalovirus infection. Circulation **92**:2594–2604.
19. **Lemstrom KB, Bruning JH, Bruggeman CA, Lautenschlager IT, Hayry PJ.** 1993. Cytomegalovirus infection enhances smooth muscle cell proliferation and intimal thickening of rat aortic allografts. J. Clin. Invest. **92**:549–558.
20. **Liu Y, Biegalke BJ.** 2002. The human cytomegalovirus UL35 gene encodes two proteins with different functions. J. Virol. **76**:2460–2468.
21. **Melnychuk RM, et al.** 2004. Human cytomegalovirus-encoded G protein-coupled receptor US28 mediates smooth muscle cell migration through G{alpha}12. J. Virol. **78**:8382–8391.
22. **Melter M, McMahon G, Fang J, Ganz P, Briscoe DM.** 1999. Current understanding of chemokine involvement in allograft transplantation. Pediatr. Transplant. **3**:10–21.
23. **Noda S, et al.** 2006. Cytomegalovirus MCK-2 controls mobilization and recruitment of myeloid progenitor cells to facilitate dissemination. Blood **107**:30–38.

24. **Orloff SL.** 1999. Elimination of donor-specific alloreactivity by bone marrow chimerism prevents cytomegalovirus accelerated transplant vascular sclerosis in rat small bowel transplants. J. Clin. Virol. **12**:142.

25. **Orloff SL, et al.** 2011. Cytomegalovirus latency promotes cardiac lymphoid neogenesis and accelerated allograft rejection in CMV naive recipients. Am. J. Transplant. **11**:45–55.

26. **Orloff SL, et al.** 2002. Elimination of donor-specific alloreactivity prevents cytomegalovirus-accelerated chronic rejection in rat small bowel and heart transplants. Transplantation **73**:679–688.

27. **Orloff SL, et al.** 1999. A rat small bowel transplant model of chronic rejection: histopathologic characteristics. Transplantation **68**:766–779.

28. **Orloff SL, et al.** 2000. Tolerance induced by bone marrow chimerism prevents transplant vascular sclerosis in a rat model of small bowel transplant chronic rejection. Transplantation **69**:1295–1303.

29. **Penfold ME, et al.** 1999. Cytomegalovirus encodes a potent alpha chemokine. Proc. Natl. Acad. Sci. U. S. A. **96**:9839–9844.

30. **Posavad CM, Newton JJ, Rosenthal KL.** 1994. Infection and inhibition of human cytotoxic T lymphocytes by herpes simplex virus. J. Virol. **68**:4072–4074.

31. **Rollins BJ.** 1997. chemokines. Blood **90**:909–928.

32. **Russel ME, Hancock WW, Wallace AF, Wyner LR, Karnovsky MJ.** 1995. Modulation of inflammatory activation pathways in the Lewis-to-F344 rat chronic cardiac rejection model. Transplant. Proc. **27**:2100–2104.

33. **Saederup N, Aguirre SA, Sparer TE, Bouley DM, Mocarski ES.** 2001. Murine cytomegalovirus CC chemokine homolog MCK-2 (m131-129) is a determinant of dissemination that increases inflammation at initial sites of infection. J. Virol. **75**:9966–9976.

34. **Saederup N, Lin YC, Dairaghi DJ, Schall TJ, Mocarski ES.** 1999. Cytomegalovirus-encoded beta chemokine promotes monocyte-associated viremia in the host. Proc. Natl. Acad. Sci. U. S. A. **96**:10881–10886.

35. **Skelton NJ, Quan C, Reilly D, Lowman H.** 1999. Structure of a CXC chemokine-receptor fragment in complex with interleukin-8. Structure **7**:157–168.

36. **Söderberg-Naucler C, Fish KN, Nelson JA.** 1997. Interferon-gamma and tumor necrosis factor-alpha specifically induce formation of cytomegalovirus-permissive monocyte-derived macrophages that are refractory to the antiviral activity of these cytokines. J. Clin. Invest. **100**:3154–3163.

37. **Söderberg-Naucler C, Fish KN, Nelson JA.** 1997. Reactivation of latent human cytomegalovirus by allogeneic stimulation of blood cells from healthy donors. Cell **91**:119–126.

38. **Söderberg-Naucler C, Nelson JY.** 1999. Human cytomegalovirus latency and reactivation—a delicate balance between the virus and its host's immune system. Intervirology **42**:314–321.

39. **Söderberg-Naucler C, et al.** 2001. Reactivation of latent human cytomegalovirus in CD14(+) monocytes is differentiation dependent. J. Virol. **75**:7543–7554.

40. **Straschewski S, et al.** 2011. Protein pUL128 of human cytomegalovirus is necessary for monocyte infection and blocking of migration. J. Virol. **85**:5150–5158.

41. **Streblow DN, et al.** 2003. Cytomegalovirus-mediated upregulation of chemokine expression correlates with the acceleration of chronic rejection in rat heart transplants. J. Virol. **77**:2182–2194.

42. **Streblow DN, et al.** 2008. The role of angiogenic and wound repair factors during CMV-accelerated transplant vascular sclerosis in rat cardiac transplants. Am. J. Transplant. **8**:277–287.

43. **Streblow DN, et al.** 2005. Rat cytomegalovirus-accelerated transplant vascular sclerosis is reduced with mutation of the chemokine-receptor R33. Am. J. Transplant. **5**:436–442.

44. **Streblow DN, et al.** 1999. The human cytomegalovirus chemokine receptor US28 mediates vascular smooth muscle cell migration. Cell **99**:511–520.

45. **Streblow DN, et al.** 2007. Rat cytomegalovirus gene expression in cardiac allograft recipients is tissue specific and does not parallel the profiles detected in vitro. J. Virol. **81**:3816–3826.

46. **Streblow DN, et al.** 2003. Human cytomegalovirus chemokine US28 induced SMC migration is mediated by focal adhesion kinase and Src. J. Biol. Chem. **278**:50456–50465.

47. **Vink C, Smit MJ, Leurs R, Bruggeman CA.** 2001. The role of cytomegalovirus-encoded homologs of G protein-coupled receptors and chemokines in manipulation of and evasion from the immune system. J. Clin. Virol. **23**:43–55.

48. **Vliegen I, et al.** 2004. Cytomegalovirus infection aggravates atherogenesis in apoE knockout mice by both local and systemic immune activation. Microbes Infect. **6**:17–24.

49. **Vliegen I, Duijvestijn A, Stassen F, Bruggeman C.** 2004. Murine cytomegalovirus infection directs macrophage differentiation into a pro-inflammatory immune phenotype: implications for atherogenesis. Microbes Infect. **6**:1056–1062.

50. **Vliegen I, Stassen F, Grauls G, Blok R, Bruggeman C.** 2002. MCMV infection increases early T-lymphocyte influx in atherosclerotic lesions in apoE knockout mice. J. Clin. Virol. **25**(Suppl. 2):S159–S171.

51. **Vomaske J, et al.** 2009. Differential ligand binding to a human cytomegalovirus chemokine receptor determines cell type-specific motility. PLoS Pathog. **5**:e1000304. doi:10.1371/journal.ppat.1000304.

52. **Wang D, Bresnahan W, Shenk T.** 2004. Human cytomegalovirus encodes a highly specific RANTES decoy receptor. Proc. Natl. Acad. Sci. U. S. A. **101**:16642–16647.

53. **Warming S, Costantino N, Court DL, Jenkins NA, Copeland NG.** 2005. Simple and highly efficient BAC recombineering using galK selection. Nucleic Acids Res. **33**:e36.

54. **Zhang YJ, Rutledge BJ, Rollins BJ.** 1994. Structure/activity analysis of human monocyte chemoattractant protein-1 (MCP-1) by mutagenesis. Identification of a mutated protein that inhibits MCP-1-mediated monocyte chemotaxis. J. Biol. Chem. **269**:15918–15924.

55. **Zhu JY, et al.** 2009. Identification of novel Epstein-Barr virus micro-RNA genes from nasopharyngeal carcinomas. J. Virol. **83**:3333–3341.